tion process). During calcification, Pi increased the rate of apoptotic cell death detected by terminal deoxyribonucleotidyl transferase-mediated dUTP-digoxigenin nick-end labeling (TUNEL) assay (Figure 2A). Furthermore, cytoplasmic histone-associated DNA fragments determined by ELISA, as a quantitative index of apoptosis, were also increased by Pi in a concentration- and time-dependent manner in both short-term (Figure 2B) and long-term conditions (supplemental Figure I). In addition, caspase 3 activation, detected by immunoblotting, by 2.6 mmol/L Pi was observed in short-term and long-term conditions (data not shown). To investigate the relationship between apoptosis and calcification, we used ZVAD.fmk, a general caspase inhibitor. We found that ZVAD.fmk significantly inhibited Pi-induced apoptosis as well as calcification in a concentration-dependent manner (Figure 2C).

It has been reported that sodium-dependent phosphate cotransporter (NPC) activity is an important pathway regulating Pi-induced HASMC calcification.[25] We confirmed that type III NPC (Pit-1) was expressed in the HASMC that we used, and its activity was enhanced by Pi treatment. Furthermore, a specific inhibitor of NPC, phosphonoformic acid (PFA), inhibited Ca deposition (reduced by 90.4% at 0.1 μmol/L), indicating that NPC-mediated Pi uptake is also essential for HASMC calcification.

To investigate the mechanisms of these statins, we examined the effect of atorvastatin on apoptosis and NPC activity. Atorvastatin, at concentrations exerting inhibition of calcification, reduced apoptosis in a concentration-dependent manner (Figure 3A). A beneficial effect of statins was also observed in the long-term condition (supplemental Figure II). On the other hand, statins did not inhibit NPC activity induced by Pi treatment (Figure 3B).

## Downregulation of Gas6-Axl Interaction Is Associated With Pi-Induced Apoptosis

Immunoblot analysis showed that the expression of Gas6 and Axl was markedly downregulated by 2.6 mmol/L Pi in both short-term (Figure 4A) and long-term (supplemental Figure III) conditions. To further examine whether Pi affects the secretion of Gas6 by HASMC, conditioned medium was collected after Pi treatment. Gas6 production in the medium was reduced by 2.6 mmol/L Pi, along with a reduction in its intracellular expression (Figure 4B). Gas6 production was also reduced in an immunoprecipitation-immunoblotting study on day 10 (Figure 4C). Next, to investigate the role of Gas6-Axl interaction in the process of apoptosis and calcification, rhGas6 and Axl-ECD were supplemented in Pi-treated HASMC. The addition of rhGas6 significantly inhibited both Pi-induced apoptosis and calcification. Addition of Axl-ECD to block the binding of Gas6 to Axl clearly abrogated the inhibitory effect of rhGas6 (Figure 4D and 4E). These results indicate that Pi-induced apoptosis and calcification are associated with downregulation of the Gas6-Axl interaction.

## Statin-Mediated Induction of Gas6 Expression Is Dependent on mRNA Stabilization, Not on Transcription

To investigate whether the antiapoptotic effect of statins is dependent on restoration of the Gas6-Axl interaction, we first assessed the effect of statins on Gas6 expression. As shown in Figure 5A, atorvastatin increased Gas6 expression, which was downregulated by Pi at both the mRNA and protein levels. Upregulation of Gas6 expression was also observed in the long-term condition (supplemental Figure IV). Furthermore, to elucidate the mechanism of statins on restoration of Gas6 mRNA, a promoter study was undertaken. Reporter assay using the −1.9 kb Gas6-luciferase DNA construct revealed that atorvastatin did not have a significant effect on Gas6 promoter activity (supplemental Figure V), as well as mRNA expression under the condition in which it was significantly inhibited by PDGF-BB (data not shown). Next, we investigated the effect of atorvastatin on mRNA stabilization using an RNA polymerase inhibitor, actinomycin D (ActD). As shown in Figure 5B, Gas6 mRNA expression was more stable in the presence of atorvastatin than in its absence under Pi and ActD treatment. The half-life was 15.9 hours with atorvastatin and 5 hours without atorvastatin, suggesting the capacity of statins to improve Gas6 mRNA stabilization (Figure 5C). Taken together, these findings suggest that the restoration of Gas6 mRNA by statins appears to be mediated by decreasing the mRNA degradation rate, and not by stimulating transcriptional activity.

Furthermore, to determine whether Gas6 is required for statin-mediated effects, we tried to knock down the action of

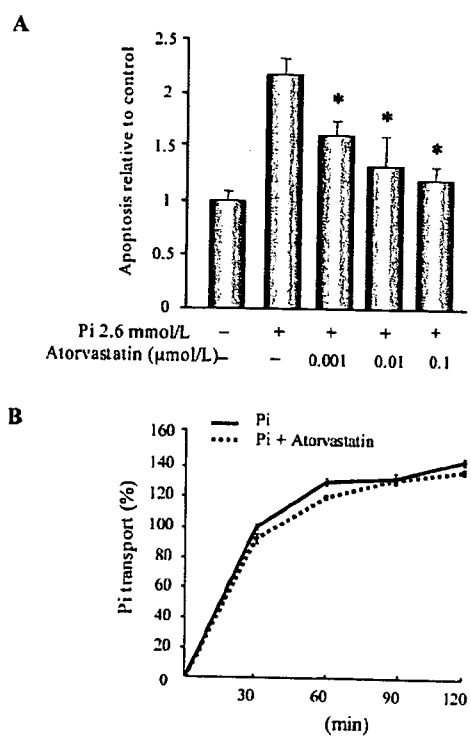


**Figure 3.** Effect of atorvastatin on Pi-induced apoptosis and NPC activity. A, HASMC were cultured with the indicated concentration of atorvastatin for 12 hours and then incubated with 2.6 mmol/L Pi for an additional 24 hours. All values are presented as mean±SEM (n=3). *$P<0.05$ vs 2.6 mmol/L Pi, statin (-) by Fisher's test. B, HASMC were treated with (dotted line) or without (solid line) 0.1 μmol/L atorvastatin in the presence of 2.6 mmol/L Pi. On day 6, NPC activity was determined in Earl's balanced salt solution containing 0.1 mmol/L $H_3{}^{32}PO_4$ (1 μCi/mL) with 143 mmol/L sodium chloride for the indicated period. All values are presented as mean±SEM (n=6).

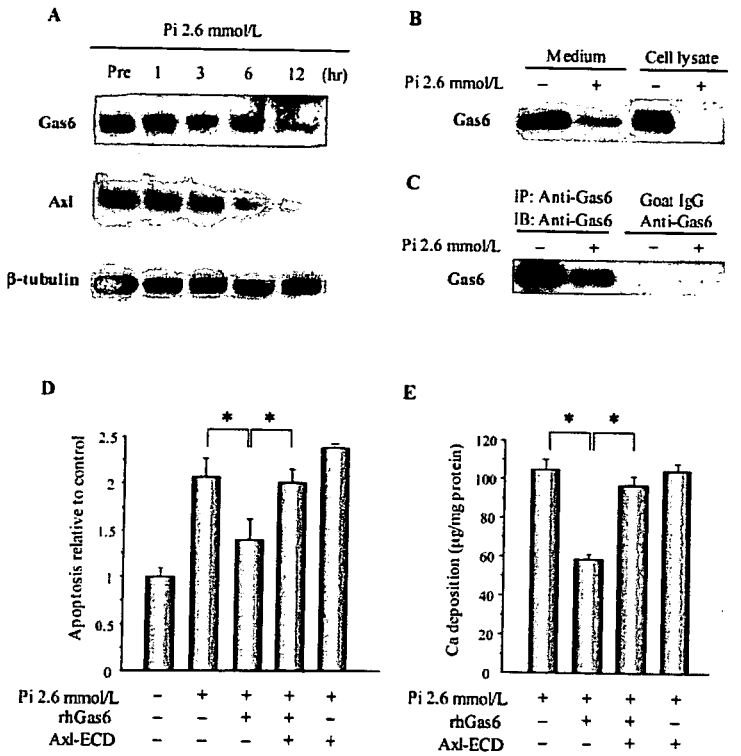


**Figure 4.** Pi reduces production of Gas6 and Axl, and rhGas6 inhibits Pi-induced apoptosis and calcification via Axl. A, HASMC were cultured in the presence of 2.6 mmol/L Pi for 12 hours. Cell lysates were subjected to SDS-PAGE followed by immunoblotting with antibodies to Gas6, Axl, or β-tubulin. B, Conditioned medium of HASMC in the absence (lane 1) or presence (lane 2) of 2.6 mmol/L Pi at 12 hours was concentrated and separated by SDS-PAGE along with cell lysates. C, Conditioned medium of HASMC on day 10 in the absence (lanes 1 and 3) or presence (lanes 2 and 4) of 2.6 mmol/L Pi was subjected to immunoprecipitation with anti-Gas6 antibody (lanes 1 and 2) or control goat IgG (lanes 3 and 4). Precipitates were immunoblotted with anti-Gas6 antibody. D, After pretreatment with rhGas6 (400 ng/mL) with or without Axl-ECD (1 μg/mL), apoptosis was induced by 2.6 mmol/L Pi. All values are presented as mean±SEM (n=3). *$P<0.05$ by Fisher's test. E, For measurement of Ca deposition, HASMC were cultured with rhGas6 (400 ng/mL) with or without Axl-ECD (1 μg/mL) in the presence of 2.6 mmol/L Pi for 6 days. All values are presented as mean±SEM (n=6). *$P<0.05$ by Fisher's test. Experiments were performed with at least 3 different cell populations.

Gas6 and examined the effect of atorvastatin on Pi-induced apoptosis and calcification. Transfection of Gas6 siRNA markedly decreased Gas6 expression in the short-term and long-term conditions (Figure 6A). The inhibitory effect of atorvastatin on Pi-induced apoptosis and calcification was reversed by Gas6 siRNA (Figure 6B and 6C). Similarly, the beneficial effect of atorvastatin was also abolished by blocking the binding of Gas6 to Axl using Axl-ECD (Figure 6D and 6E). These data support a critical role of Gas6 in the preventive effect of statins on apoptosis and calcification.

## Discussion

The present study demonstrated that statins protected HASMC from Pi-induced calcification. The clinical effect of statins on vascular calcification is controversial. Many retrospective clinical studies[6,7,9] and a prospective study[8] have shown beneficial effects, whereas recent prospective studies were unable to show such effects.[12,13] The reason is not yet clear, and the time window of statin use has been raised as an important matter. The discrepancy may also derive from the complex in vivo effects of statins. In this regard, it is important to analyze the detailed regulatory mechanism of statins in a simple model.

In Pi-induced calcification, HASMC undergo apoptosis. A causal link between apoptosis and calcification was evident from the finding that both apoptosis and calcification were inhibited by the general caspase inhibitor, ZVAD.fmk. As reported previously,[25] we confirmed that NPC-mediated Pi uptake is another essential mechanism for HASMC calcification. Given that apoptosis does not always lead to calcification, Pi-induced HASMC calcification is presumably dependent on both an NPC-mediated phenotypic transition from SMC to an osteoblastic phenotype and apoptotic cell death. With respect to the mechanism of action of statins, they clearly inhibited Pi-induced apoptosis, although they did not have an effect on Pi-induced NPC activity or osteoblastic differentiation; Pi-induced upregulation of matrix Gla protein (MGP) mRNA was not inhibited by atorvastatin (supplemental Figure VI). These results suggest that apoptosis is the target of statins in inhibiting HASMC calcification.

Another important signal in Pi-induced calcification is an increase in intracellular Ca ($[Ca^{2+}]_i$). Statins have been shown to inhibit VSMC proliferation[5] and reduce the acute increase of $[Ca^{2+}]_i$ in a mevalonate and isoprenoid pathway–independent manner.[26] On the other hand, $[Ca^{2+}]_i$ is reported to modulate Pi-induced apoptosis of terminally differentiated chondrocytes.[27] Therefore, modulation of $[Ca^{2+}]_i$ is another possible mechanism of the inhibition of apoptosis by statins. In this study, we investigated the association of proliferation with Pi-induced apoptosis and calcification. We found that Pi did not affect proliferation, measured by the incorporation of 5-bromo-2′-deoxyuridine (BrdU) during calcification (data not shown). We also found that the inhibitory effect of statins on calcification was not affected by an inhibitor of Rho kinase (Y-27632), an important modulator of the mevalonate and isoprenoid pathway affecting proliferation and apoptosis (supplemental Figure VII). These results suggest that proliferation is not associated with Pi-induced calcification. The inhibitory effect of statins on calcification was not blocked by mevalonate, farnesylpyrophosphate, geranylgeranylpyrophosphate, or Rho kinase inhibitor, suggesting that the effect of statins is not dependent on the mevalonate and isoprenoid pathways. Indeed, a mevalonate pathway–independent effect of statins has been reported previously,[26,28–30] although the precise mechanism has not been shown. The pleiotropism of statins is of continuing interest.

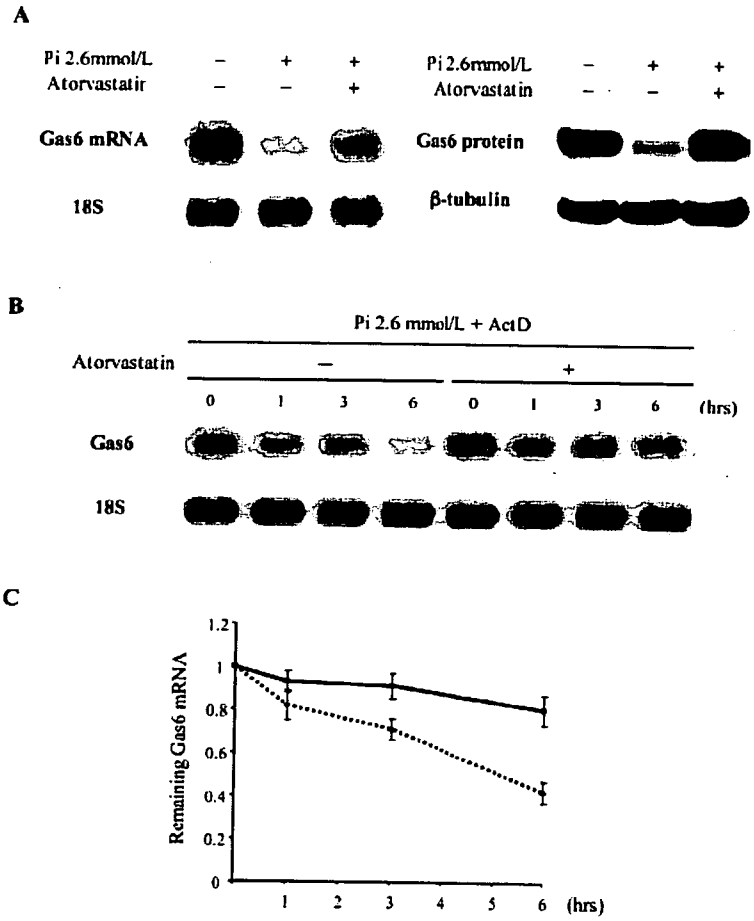


Figure 5. Atorvastatin enhances Gas6 mRNA stabilization, but not transcription. A, After pretreatment with atorvastatin (0.1 μmol/L) for 12 hours, apoptosis was induced by 2.6 mmol/L Pi. At 12 hours, mRNA was isolated and Northern blot analysis for Gas6 and 18S was performed. Simultaneously, cell lysates were collected and subjected to SDS-PAGE followed by immunoblotting with antibodies to Gas6 and β-tubulin. B, Serum-starved HASMC were incubated with actinomycin D (Act D) (5 μg/mL) in the presence of 2.6 mmol/L Pi after 12 hours of atorvastatin (0.1 μmol/L) treatment. Total RNA was harvested at 0, 1, 3, and 6 hours for Northern blot analysis. C, Signal density of Gas6 mRNA with (solid line) or without (dotted line) atorvastatin (0.1 μmol/L) in the presence of 2.6 mmol/L Pi and Act D (5 μg/mL) was normalized to that of 18S RNA at each time point. Gas6 mRNA level at time 0 was given the value 1. Each experiment was performed in triplicate for each condition.

An antiapoptotic effect of statins has been shown in various cell types.[31–34] In cardiomyocytes, apoptosis induced by hypoxia or protein kinase C (PKC) inhibitors was inhibited by 10 μmol/L pravastatin or 0.1 μg/mL atorvastatin, respectively.[31,32] Simvastatin (1 μmol/L) promoted endothelial cell survival.[33] In VSMC, 7-ketocholesterol–induced apoptosis was inhibited by 10 μmol/L pravastatin.[34] However, in contrast to the results of the present and other studies, a proapoptotic effect of statins has also been reported in VSMC,[35] endothelial cells,[36] and cardiac myocytes.[37] Although the precise mechanism is not understood, it can be postulated that statins have biphasic effects on cell survival (an antiapoptotic effect at low concentrations and a proapoptotic effect at high concentrations) depending on the type of cell, statins, and apoptotic stimulus. Indeed, Weis et al showed dose-dependent biphasic effects of statins on apoptotic activity in microvascular endothelial cells.[30] Consistent with these data, we found that 3 different statins displayed an antiapoptotic effect at low concentrations and a proapoptotic effect at high concentrations (>1 μmol/L for atorvastatin and fluvastatin; >100 μmol/L for pravastatin) (data not shown).

During Pi-induced apoptosis, we have shown that Pi downregulates the Gas6-Axl interaction, resulting in blockade of a survival signal, thereby promoting apoptosis and calcification. We previously proposed that Gas6 may allow Axl-expressing phagocytic cells, eg, macrophages and VSMC, to recognize cells exposing phosphatidylserine (PS) on the outer cell membrane, the initial step of the apoptotic process.[38] Proudfoot et al also showed that in vascular calcification, several PS-exposing cells are observed within and on the periphery of the nodules.[16] PS exposure by apoptotic bodies generates a potential Ca-binding site and membrane surface suitable for hydroxyapatite deposition.[39,40] Based on these observations, Gas6-Axl downregulation is presumably involved in decreased cell survival and clearance, both directing cells to apoptosis-mediated mineral deposition.

With regard to the molecular pathway of the restoration of Gas6 by statins, we have shown that statins retarded degradation of Gas6 mRNA, not increasing the transcriptional rate. Indeed, it was reported that statins improve mRNA stability as well as transcription.[41,42] In addition, the result that suppression of the action of Gas6 by siRNA and Axl-ECD abrogated the inhibitory effect of statins on apoptosis and inhibition clearly indicates a pivotal role of Gas6 in the effect of statins.

We conclude that statins inhibit Pi-induced HASMC calcification by preventing apoptosis via restoration of the Gas6-Axl pathway. The regulation of Gas6 by statins occurs at the posttranscriptional level. The present study provides evidence of a preventive role of statins in vascular calcification and further indicates the pleiotropic effects of statins, which could potentially contribute to the treatment of cardiovascular disease.

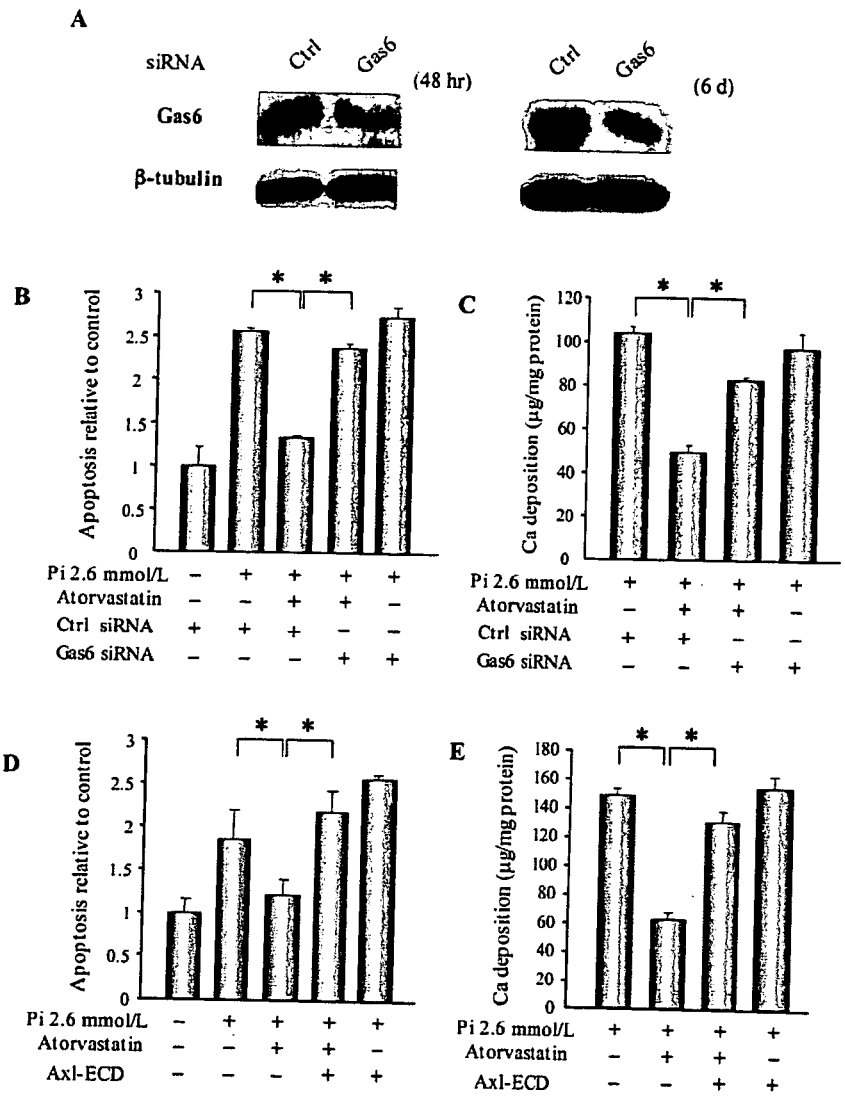


**Figure 6.** Gas6 knockdown abolishes inhibition of Pi-induced apoptosis and calcification by atorvastatin. A, Gas6-specific siRNA (100 nmol/L) and nonspecific siRNA (Ctrl siRNA) were transfected into HASMC, and immunoblotting was performed at 48 hours and 6 days after transfection. B, Serum-starved HASMC were transfected with 100 nmol/L Gas6 siRNA and control (Ctrl) siRNA. After transfection, cells were treated with atorvastatin (0.1 μmol/L) for 12 hours, then with 2.6 mmol/L Pi for an additional 24 hours before measurement of apoptosis (n=3). C, For measurement of Ca deposition, HASMC were transfected with 100 nmol/L Gas6 siRNA and control siRNA and incubated with atorvastatin (0.1 μmol/L) and 2.6 mmol/L Pi for 6 days (n=3). D, In the case of Axl-ECD, HASMC were pretreated with atorvastatin (0.1 μmol/L) and Axl-ECD (1 μg/mL) for 12 hours, then incubated with 2.6 mmol/L Pi for an additional 24 hours. Thereafter, a quantitative index of apoptosis was determined by ELISA (n=3). E, HASMC were cultured with atorvastatin (0.1 μmol/L) and Axl-ECD (1 μg/mL) in the presence of 2.6 mmol/L Pi for 6 days. Ca content was measured and normalized by cell protein content. All values are presented as mean±SEM (n=6). *$P<0.05$ by Fisher's test. Each panel shows a representative example of 3 independent experiments.

## Acknowledgments

This study was supported by a grant-in-aid for scientific research from the Ministry of Education, Science, Sports, and Culture of Japan (grant 15390239) and by the Mitsui Sumitomo Insurance Welfare Foundation, the Ono Medical Research Foundation, the Kanzawa Medical Research Foundation, the Novartis Foundation for Gerontrogical Research, and the Takeda Research Foundation. We thank Yuki Ito for technical assistance.

## References

1. Eggen DA. Relationship of calcified lesions to clinically significant atherosclerotic lesions. *Ann N Y Acad Sci.* 1968;149:752–767.
2. Wexler L, Brundage B, Crouse J, Detrano R, Fuster V, Maddahi J, Rumberger J, Stanford W, White R, Taubert K. Coronary artery calcification: pathophysiology, epidemiology, imaging methods, and clinical implications. A statement for health professionals from the American Heart Association Writing Group. *Circulation.* 1996;94:1175–1192.
3. Mullen MJ, Wright D, Donald AE, Thorne S, Thomson H, Deanfield JE. Atorvastatin but not L-arginine improves endothelial function in type-I diabetes mellitus: a double-blind study. *J Am Coll Cardiol.* 2000;36:410–416.
4. Bustos C, Hernandez-Presa MA, Ortego M, Tunon J, Ortega L, Perez F, Diaz C, Hernandez G, Egido J. HMG-CoA reductase inhibition by atorvastatin reduces neointimal inflammation in a rabbit model of atherosclerosis. *J Am Coll Cardiol.* 1998;32:2057–2064.
5. Axel DI, Riessen R, Runge H, Viebahn R, Karsch KR. Effects of cerivastatin on human arterial smooth muscle cell proliferation and migration in transfilter cocultures. *J Cardiovasc Pharmacol.* 2000;35:619–629.
6. Shavelle DM, Takasu J, Budoff MJ, Mao S, Zhao XQ, O'Brien KD. HMG CoA reductase inhibitor (statin) and aortic valve calcium. *Lancet.* 2002;359:1125–1126.
7. Novaro GM, Tiong IY, Pearce GL, Lauer MS, Sprecher DL, Griffin BP. Effect of hydroxymethylglutaryl coenzyme A reductase inhibitors on the progression of calcific aortic stenosis. *Circulation.* 2001;104:2205–2209.
8. Achenbach S, Ropers D, Pohle K, Leber A, Thilo C, Knez A, Menendez T, Maeffert R, Kusus M, Regenfus M, Bickel A, Haberl R, Steinbeck G, Moshage W, Daniel WG. Influence of lipid-lowering therapy on the progression of coronary artery calcification: a prospective evaluation. *Circulation.* 2002;106:1077–1082.
9. Callister TQ, Raggi P, Cooil B, Lippolis NJ, Russo DJ. Effect of HMG-CoA reductase inhibitors on coronary artery disease as assessed by electron-beam computed tomography. *N Engl J Med.* 1998;339:1972–1978.
10. Williams JK, Sukhova GK, Herrington DM, Libby P. Pravastatin has cholesterol-lowering independent effects on the artery wall of atherosclerotic monkeys. *J Am Coll Cardiol.* 1998;31:684–691.
11. Bea F, Blessing E, Bennett B, Levitz M, Wallace EP, Rosenfeld ME. Simvastatin promotes atherosclerotic plaque stability in apoE-deficient mice independently of lipid lowering. *Arterioscler Thromb Vasc Biol.* 2002;22:1832–1837.
12. Cowell SJ, Newby DE, Prescott RJ, Bloomfield P, Reid J, Northridge DB, Boon NA. A randomized trial of intensive lipid-lowering therapy in calcific aortic stenosis. *N Engl J Med.* 2005;352:2389–2397.

13. Wanner C, Krane V, Marz W, Olschewski M, Mann JF, Ruf G, Ritz E. Atorvastatin in patients with type 2 diabetes mellitus undergoing hemodialysis. *N Engl J Med.* 2005;353:238–248.
14. Goodman WG, London G, Amann K, Block GA, Giachelli C, Hruska KA, Ketteler M, Levin A, Massy Z, McCarron DA, Raggi P, Shanahan CM, Yorioka N; Vascular Calcification Work Group. Vascular calcification in chronic kidney disease. *Am J Kidney Dis.* 2004;43:572–579.
15. Giachelli CM, Jono S, Shioi A, Nishizawa Y, Mori K, Morii H. Vascular calcification and inorganic phosphate. *Am J Kidney Dis.* 2001;38: S34–S37.
16. Proudfoot D, Skepper JN, Hegyi L, Bennett MR, Shanahan CM, Weissberg PL. Apoptosis regulates human vascular calcification by apoptotic bodies. *Circ Res.* 2000;87:1055–1062.
17. Mansfield K, Rajpurohit R, Shapiro IM. Extracellular phosphate ions cause apoptosis of terminally differentiated epiphyseal chondrocytes. *J Cell Physiol.* 1999;179:276–286.
18. Collett G, Wood A, Alexander MY, Varnum BC, Boot-Handford RP, Ohanian V, Ohanian J, Fridell YW, Canfield AE. Receptor tyrosine kinase Axl modulates the osteogenic differentiation of pericytes. *Circ Res.* 2003;92:1123–1129.
19. Mark MR, Chen J, Hammonds RG, Sadick M, Godowsk PJ. Characterization of Gas6, a member of the superfamily of G domain-containing proteins, as a ligand for Rse and Axl. *J Biol Chem.* 1996;271:9785–9789.
20. Yanagita M, Arai H, Ishii K, Nakano T, Ohashi K, Mizuno K, Varnum B, Fukatsu A, Doi T, Kita T. Gas6 regulates mesangial cell proliferation through Axl in experimental glomerulonephritis. *Am J Pathol.* 2001;158: 1423–1432.
21. Goruppi S, Ruaro E, Schneider C. Gas6, the ligand of Axl tyrosine kinase receptor, has mitogenic and survival activities for serum starved NIH3T3 fibroblasts. *Oncogene.* 1996;12:471–480.
22. Nakano T, Ishimoto Y, Kishino J, Umeda M, Inoue K, Nagata K, Ohashi K, Mizuno K, Arita H. Cell adhesion to phosphatidylserine mediated by a product of growth arrest-specific gene 6. *J Biol Chem.* 1997;272: 29411–29414.
23. Fridell YW, Villa J Jr, Attar EC, Liu ET. Gas6 induces Axl-mediated chemotaxis of vascular smooth muscle cells. *J Biol Chem.* 1998;273: 7123–7126.
24. Ming Cao W, Murao K, Imachi H, Sato M, Nakano T, Kodama T, Sasaguri Y, Wong NC, Takahara J, Ishida T. Phosphatidylinositol 3-OH kinase-Akt/protein kinase B pathway mediates Gas6 induction of scavenger receptor a in immortalized human vascular smooth muscle cell line. *Arterioscler Thromb Vasc Biol.* 2001;21:1592–1597.
25. Jono S. McKee MD, Murry CE, Shioi A, Nishizawa Y, Mori K, Morii H, Giachelli CM. Phosphate regulation of vascular smooth muscle cell calcification. *Circ Res.* 2000;87:e10–e17.
26. Bergdahl A, Persson E, Hellstrand P, Sward K. Lovastatin induces relaxation and inhibits L-type Ca(2+) current in the rat basilar artery. *Pharmacol Toxicol.* 2003;93:128–134.
27. Mansfield K, Pucci B, Adams CS, Shapiro IM. Induction of apoptosis in skeletal tissues: phosphate-mediated chick chondrocyte apoptosis is calcium dependent. *Calcif Tissue Int.* 2003;73:161–172.
28. Weitz-Schmidt G, Welzenbach K, Brinkmann V, Kamata T, Kallen J, Bruns C, Cottens S, Takada Y, Hommel U. Statins selectively inhibit leukocyte function antigen-1 by binding to a novel regulatory integrin site. *Nat Med.* 2001;7:687–692.
29. Wagner AH, Gebauer M, Guldenzoph B, Hecker M. 3-Hydroxy-3-methylglutaryl coenzyme A reductase-independent inhibition of CD40 expression by atorvastatin in human endothelial cells. *Arterioscler Thromb Vasc Biol.* 2002;22:1784–1789.
30. Weis M, Heeschen C, Glassford AJ, Cooke JP. Statins have biphasic effects on angiogenesis. *Circulation.* 2002;105:739–745.
31. Bergmann MW, Rechner C, Freund C, Baurand A, El Jamali A, Dietz R. Statins inhibit reoxygenation-induced cardiomyocyte apoptosis: role for glycogen synthase kinase 3$\beta$ and transcription factor $\beta$-catenin. *J Mol Cell Cardiol.* 2004;37:681–690.
32. Tanaka K, Honda M, Takabatake T. Anti-apoptotic effect of atorvastatin, a 3-hydroxy-3-methylglutaryl coenzyme a reductase inhibitor, on cardiac myocytes through protein kinase C activation. *Clin Exp Pharm Phy.* 2004;31:360–364.
33. Kureishi Y, Luo Z, Shiojima I, Bialik A, Fulton D, Lefer DJ. Sessa WC, Walsh K. The HMG-CoA reductase inhibitor simvastatin activates the protein kinase Akt and promotes angiogenesis in normocholesterolemic animals. *Nature Med.* 2000;6:1004–1010.
34. Miyashita Y, Ozaki H, Koide N, Otsuka M, Oyama T, Itoh Y, Mastuzaka T, Shirai K. Oxysterol-induced apoptosis of vascular smooth muscle cells is reduced by HMG-CoA reductase inhibitor, pravastatin. *J Atheroscler Thromb.* 2002;9:65–71.
35. Guijarro C, Blanco-Colio LM, Ortego M, Alonso C, Ortiz A, Plaza JJ, Diaz C, Hernandez G, Egido J. 3-Hydroxy-3 methylglutaryl coenzyme A reductase and isoprenylation inhibitors induce apoptosis of vascular smooth muscle cells in culture. *Circ Res.* 1998;83:490–500.
36. Newton CJ, Ran G, Xie YX, Bilko D, Burgoyne CH, Adams I, Abidia A, McCollum PT, Atkin SL. Statin-induced apoptosis of vascular endothelial cells is blocked by dexamethasone. *J Endocrinol.* 2002;174:7–16.
37. Ogata Y, Takahashi M, Takeuchi K, Ueno S, Mano H, Ookawara S, Kobayashi E, Ikeda U, Shimada K. Fluvastatin induces apoptosis in rat neonatal cardiac myocytes: a possible mechanism of statin-attenuated cardiac hypertrophy. *J Cardiovasc Pharmacol.* 2002;40:907–915.
38. Ishimoto Y, Ohashi K, Mizuno K, Nakano T. Promotion of the uptake of PS liposomes and apoptotic cells by a product of growth arrest-specific gene, gas6. *J Biochem (Tokyo).* 2000;127:411–417.
39. Cotmore JM, Nichols G Jr, Wuthier RE. Phospholipid-calcium phosphate complex: enhanced calcium migration in the presence of phosphate. *Science.* 1971;172:1339–1341.
40. Skrtic D, Eanes ED. Membrane mediated precipitation of calcium phosphate in model liposomes with matrix vesicle-like lipid composition. *Bone Miner.* 1992;16:109–119.
41. Walter DH, Zeiher AM, Dimmeler S. Effects of statins on endothelium and their contribution to neovascularization by mobilization of endothelial progenitor cells. *Coron Artery Dis.* 2004;15:235–242.
42. Menschikowski M, Hagelgans A, Heyne B, Hempel U, Neumeister V, Goez P, Jaross W, Siegert G. Statins potentiate the IFN-gamma-induced upregulation of group IIA phospholipase A2 in human aortic smooth muscle cells and HepG2 hepatoma cells. *Biochim Biophys Acta.* 2005; 1733:157–171.

*Geriatr Gerontol Int 2006; 6: 270–273*

CASE REPORT

# Elderly patient presenting with severe thyrotoxic hypercalcemia

Reiko Kikuchi,[1] Satoru Mochizuki,[1] Masahiko Shimizu,[1] Noriko Sudoh,[1] Koichi Kozaki,[1] Masahiro Akishita[2] and Kenji Toba[1]

*[1]Department of Geriatric Medicine, Kyorin University School of Medicine, and [2]Department of Geriatric Medicine, Graduate School of Medicine, The University of Tokyo, Tokyo, Japan*

An 81-year-old woman with Graves' disease and osteoporosis was referred to the hospital because of anorexia over one month and impaired consciousness. She also presented with low-grade fever and emaciation. Laboratory tests revealed marked hypercalcemia (corrected serum calcium level of 12.4 mg/dL), which was initially suspected to result from vitamin D toxicity, because she had been taking vitamin D3 (alphacalcidol of 0.5 μg/day) for the treatment of osteoporosis. However, discontinuation of vitamin D3 and fluid infusion did not ameliorate hypercalcemia one week later. After excluding hyperparathyroidism and malignancy-related hypercalcemia, hypercalcemia was considered to be attributable to the exacerbation of hyperthyroidism (free T4 of 6.69 ng/dL, free T3 of 13.27 pg/mL and thyroid stimulating hormone (TSH) <0.015 μIU/mL) with increased bone resorption. Finally, the increased dose of thiamazole (30 mg/day) normalized serum calcium level and thyroid function three months later. Laboratory tests suggested that normal bone formation in spite of increased bone resorption contributed to hypercalcemia in hyperthyroid state.

**Keywords:** deoxypyridinoline, hypercalcemia, hyperthyroidism, osteoporosis, p-N-telopeptides of collagen cross-links.

## Introduction

Hypercalcemia has been associated in approximately 20% of the patients with hyperthyroidism, but is mild in most cases, ranging from the upper normal limit to the slightly elevated level.[1–3] Consequently, we rarely see hyperthyroidism with symptomatic hypercalcemia. Many genotypes have been associated with Graves' disease.[4] Also, a small number of studies have shown that polymorphisms in calcium-regulating genes such as calcium-sensing receptor[5] and vitamin D receptor[6] may influence calcium metabolism in adults. However, no study has reported the association of those polymorphisms with thyrotoxic hypercalcemia. More studies as well as more polymorphisms including haplotype analysis should be performed to clarify the underlying mechanism.

Here, we report an elderly patient presenting with severe symptomatic hypercalcemia resulting from hyperthyroidism.

## Case report

An 81-year-old woman was admitted to the Department of Geriatric Medicine, Kyorin University Hospital because of hypercalcemia on February 14 2004. She had Basedow's disease and osteoporosis, and had been taking thiamazole 5 mg/day and alphacalcidol 0.5 μg/day. In January 2004, anorexia had gradually developed followed by gait disturbance. When she was referred to the hospital on February 14, she also presented with confusion and low-grade fever of 37.2°C. Her blood pressure was 122/62 mmHg with a pulse rate of 98 bpm. Physical examination showed a soft diffuse goiter and a systolic ejection murmur of Levine II/VI at the apex, while abdominal and neurological findings were normal.

Accepted for publication 15 March 2006.

Correspondence: Dr Kenji Toba, MD, PhD, Department of Geriatric Medicine, Kyorin University School of Medicine, 6-20-2 Shinkawa, Mitaka, Tokyo 181-8611, Japan. Email: toba@kyorin-u.ac.jp

 doi: 10.1111/j.1447-0594.2006.00359.x 

**Table 1** Laboratory tests on admission

| Test | Result |
|---|---|
| Hb | 10.5 g/dL |
| Ht | 32.6% |
| RBC | $367 \times 10^4/\mu L$ |
| PLT | $22.2 \times 10^4/\mu L$ |
| WBC | 3200/μL |
| Na | 144 mEq/L |
| K | 3.1 mEq/L |
| Cl | 100 mEq/L |
| Ca | 11.7 mg/dL |
| IP | 3.4 mg/dL |
| BUN | 19.3 mg/dL |
| Cr | 0.7 mg/dL |
| TP | 6.4 g/dL |
| Alb | 3.3 g/dL |
| ALP | 226 IU/L |
| AST | 37 IU/L |
| ALT | 35 IU/L |
| LDH | 333 U/L |
| CK | 25 IU/L |
| Glu | 126 mg/dL |
| CRP | 0.2 mg/dL |

Alb, albumin; ALP, alkaline phosphatase; ALT, alkaline aminotransferase; AST, asparate aminotransferase; BUN, blood urea nitrogen; CK, creatine kinase; CRP, C-reactive protein; LDH, lactate dehydrogenase; PLT, platelet; RBC, red blood cell count; TP, total protein; WBC, white blood cell count.

**Table 2** Results of thyroid function test

| Test | Result (normal range) |
|---|---|
| FreeT4 | 6.69 ng/dL (0.73–1.53) |
| FreeT3 | 13.27 pg/mL (1.63–3.20) |
| Thyroid stimulating hormone (THS) | 0.015 IU/mL (0.41–5.27) |
| TSH receptor antibody | 51.2% (15<) |
| TSAb (thyroid stimulatory antibody) | 540% (180<) |
| Antithyroid peroxydase antibody | 43.8 U/mL (0.3<) |
| Serum thyroglobulin autoantibodies | 0.3 < U/mL (0.3<) |

On laboratory tests (Table 1), she showed blood hemoglobin of 10.5 g/dL, white blood cell counts of 3200/μL and serum calcium of 11.7 mg/dL (corrected calcium of 12.4 mg/dL). Other electrolytes as well as liver and kidney function were normal. Thyroid function tests (Table 2) revealed marked hyperthyroidism; free T4 of 6.69 (reference, 0.90–1.70) ng/dL, free T3 of 13.27 (2.3–4.3) pg/mL and thyroid stimulating hormone (TSH) of <0.015 (0.5–5.0) μIU/mL. Plasma levels of TSH receptor antibody, thyroid stimulating antibody and anti-TPO antibody were elevated, compatible with the findings in Graves' disease. Plasma intact PTH was 13 (10–65) pg/mL and PTH-related protein was not detected.

**Table 3** Results of markers of bone metabolism

| Marker | Result (normal range) |
|---|---|
| Osteocalcin | 9.5 ng/mL (2.5–13) |
| Bone-specific alkaline phosphatase | 24.2 U/L (9.6–35.4) |
| p-N-telopeptides | 43.3 nMBCE/L (10.7–24.0) |
| Deoxypyridinoline/Cr | 43.8 nmol/L/nMCr (2.8–7.6) |
| calcitonin | 33 pg/mL |
| 1–25(OH)Vit$D_3$ | 6 pg/mL (20–60) |

**Figure 1** X-ray of lumbar vertebrae.

As shown in Table 3, markers of bone resorption such as deoxypyridinoline (DPD) and N-telopeptides of collagen cross-links (NTx) were elevated, whereas those of bone formation such as osteocalcin and bone-type alkaline phosphatase were not. Bone mineral density of lumbar vertebrae was −3.29 (T score), and that of femur was −3.72 (T score). Multiple compression fractures and remarkable reduction in bone mineral density were found on spinal lateral X-rays and dual energy X-ray absorptiometry, respectively (Fig. 1).

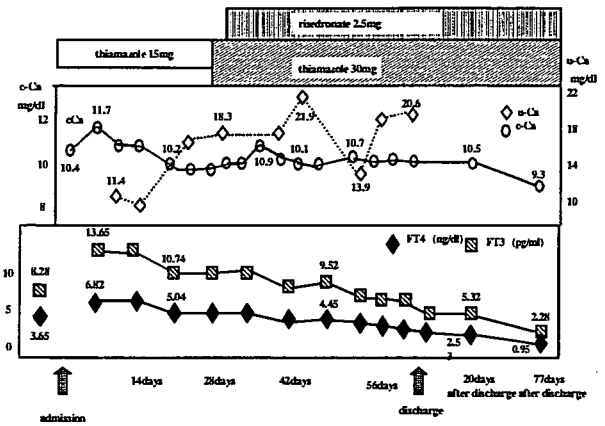


**Figure 2** Clinical course of the patient. Thyroid stimulating hormone (TSH) was below the detection limit throughout the clinical course. c-Ca, collected serum calcium; u-Ca, urinary calcium; FT4, free thyroxine; FT3, free triiodothyronine.

Initially, vitamin D toxicity was suspected as a cause of hypercalcemia; thus, alphacalcidol was ceased with fluid infusion to wash out calcium. However, the hypercalcemia had not improved one week later. Laboratory and imaging tests were carried out to exclude hyperparathyroidism, humoral hypercalcemia of malignancy, osteolytic bone metastases and multiple myeloma. Finally, hypercalcemia was considered to be attributable to the exacerbation of hyperthyroidism with high bone turnover. Consequently, the dose of thiamazole was increased to 30 mg/day to normalize thyroid function. As shown in Figure 2, free T4 and free T3, as well as serum calcium were gradually decreased, and the patient was discharged on May 14 2004. In August 2004, her thyroid function returned to normal (free T4 of 0.95 ng/dL and free T3 of 2.28 pg/mL) with corrected serum calcium concentration of 9.2 mg/dL.

## Discussion

Hypercalcemia associated with hyperthyroidism has been reported to occur more frequently in elderly patients than in younger patients; the incidence of hypercalcemia was 2.3% in hyperthyroid patients under 60 years of age and was 18.8% in those over 60 years of age.[2] The severity of hypercalcemia, however, is generally mild, ranging from the upper normal limit to the slightly elevated level,[3] and other complications should be suspected when serum calcium concentration is over 12 mg/dL[7] Actually, case reports have shown that hyperparathyroidism is uncommonly associated with hypercalcemia in thyrotoxicosis.[8] Only several cases have been reported that hyperthyroidism was considered the only cause of hypercalcemia over 12.0 mg/dL[9–11] In our case, laboratory tests and diagnostic imaging excluded hyperparathyroidism as well as malignant neoplasms. Furthermore, hypercalcemia was ameliorated in parallel with the improvement of hyperthyroidism, indicating that hypercalcemia resulted from hyperthyroidism.

Thyroid hormones play a critical role in bone development because hypothyroidism in childhood results in the impaired skeletal development.[12] In adults, thyroid hormones are important in the maintenance of bone mass. Thyroid hormone receptors are expressed in bone cells such as osteoblasts and osteoclasts.[12] In adult hyperthyroidism, there is increased bone remodelling, characterized by an increase in both bone resorption and formation, and an imbalance between bone resorption and formation, which results in bone loss and an increased risk for osteoporotic fracture.[12] In our case, however, the markers of bone resorption were elevated but those of bone formation were not. This pattern is consistent with the changes of bone metabolism in older osteoporotic patients,[13] but is different from that in hyperthyroidism as mentioned above. This might be due to the age-related decline in thyroid hormone signaling that leads to bone formation. However, no reports including animal experiments to support this hypothesis can be found so far. This should be investigated in the future.

Anti-thyroid drugs restore not only serum calcium levels[14] but also bone mineral density[15] in patients with thyrotoxic hypercalcemia. It has been also reported that a β blocker, propranolol,[16,17] and radioiodine therapy[10] may ameliorate thyrotoxic hypercalcemia. In our case, an increased dose of thiamazole normalized both thyroid function and serum calcium levels several months later, but bone mineral density was not increased. Longer time periods would be necessary to see the recovery of bone mass if possible.

## References

1 Daniel T, Aran B. The skeletal system in thyrotoxicosis. In: Lewis EB, Robert DU, (eds). *Werner and Ingbar's the Thyroid*, 8th edn. Philadelphia, PA: A Wolters Kluwer Co., 2000; 659–666.
2 Szabo ZS, Ritzl F. Hypercalcemia in hyperthyroidism. Role of age and goiter type. *Klin Wochenschr* 1981; **59**: 275–279.
3 Mosekilde L, Melsen F, Bagger JP *et al.* Bone changes in hyperthyroidism: interrelationships between bone morphometry, thyroid function and calcium-phosphorus metabolism. *Acta Endocrinol* 1977; **85**: 515–525.
4 Dittmar M, Kahaly GJ. Immunoregulatory and susceptibility genes in thyroid and polyglandular autoimmunity. *Thyroid* 2005; **15**: 239–250.
5 Cole DE, Vieth R, Trang HM *et al.* Association between total serum calcium and the A986S polymorphism of the calcium-sensing receptor gene. *Mol Genet Metab* 2001; **72**: 168–174.
6 Akcay A, Ozdemir FN, Sezer S *et al.* Association of vitamin D receptor gene polymorphisms with hypercalcemia in

peritoneal dialysis patients. *Perit Dial Int* 2005; **25**: S52–S55.
7 Ryo M, Shigeru Y, Hyo ES *et al.* The parathyroid function in patients with hyperthyroidism. *Nippon Naibunpi Gakkai Zasshi* 1984; **60**: 892–898.
8 Maxon HR, Apple DJ, Goldsmith RE. Hypercalcemia in thyrotoxicosis. *Surg Gynecol Obstet* 1987; **147**: 694–696.
9 Inaba M, Hamada N, Itoh K *et al.* A case report on disequilibrium hypercalcemia in hyperthyroidism. Comparison of calcium metabolism with other patients with hyperthyroidism. *Endocrinol Jpn* 1982; **29**: 389–393.
10 Akihan Z, Singh A. Hyperthyroidism manifested as hypercalcemia. *South Med J* 1996; **89**: 997–998.
11 Reular JB, Wise RW, Thorpe JB. Anemia, renal insufficiency, and hypercalcemia in a man with hyperthyroidism. *South Med J* 1985; **78**: 59–63.
12 Bassett JH, Williams GR. The molecular actions of thyroid hormone in bone. *Trends Endocrinol Metab* 2003; **14**: 356–364.
13 Chan GK, Duque G. Age-related bone loss: old bone, new facts. *Gerontology* 2002; **48**: 62–71.
14 Hedman I, Tisell LE. Life-threatening hypercalcemia in a case of thyrotoxicosis: clinical features and management. A case report. *Acta Chir Scand* 1985; **151**: 487–489.
15 Diamond T, Julie V, Richard S, Ptrick B. Thyrotoxic bone disease in women: a potentially reversible disorder. *Ann Intern Med* 1994; **120**: 8–11.
16 Shahshahani MN, Palmieri GM. Oral propranolol in hypercalcemia associated with apathetic thyrotoxicosis. *Am J Med Sci* 1978; **275**: 199–202.
17 Mallette LE, Rubenfeld S, Silverman V. A controlled study of the effects of thyrotoxicosis and propranolol treatment on mineral metabolism and parathyroid hormon immunoreactivity. *Metabolism* 1985; **34**: 999–1006.

〈原　著〉

# 超高齢者におけるクレアチニンクリアランス推定式の比較検討

平山　俊一[1)]　菊池　令子[2)]　井上慎一郎[2)]　塚原　大輔[2)]　末光　有美[2)]
小林　義雄[2)]　杉山　陽一[2)]　長谷川　浩[2)]　神崎　恒一[2)]　井上　剛輔[3)]
鳥羽　研二[2)]

**要　約**　**目的**：高齢患者は外来では24時間クレアチニンクリアランスの測定が困難であり，服用薬物数も多いため，クレアチニンクリアランス実測値をできるだけ正確に反映する推定式を利用することは臨床上重要である．**対象**：各種基礎疾患を有する85歳以上の超高齢者67名を含む入院高齢者143名（男性73名　女性70名　平均年齢82.9±8.6歳）．**方法**：4種のクレアチニンクリアランス推定式から得られた推定値と24時間クレアチニンクリアランスの実測値との相関を比較検討した．**結果と結論**：全体として今回の検討では超高齢者においてもCockcroft and Gaultの式による推定値が最もよい相関を示した．85歳以上の女性超高齢者において実測値と推定式の相関が低く，推定式の改定についても今後の検討課題と思われる．

**Key words**：超高齢者，クレアチニンクリアランス，推定式，Cockcroft and Gaultの式，安田の式

（日老医誌　2007；44：90–94）

## 緒　言

高齢社会の到来により，外来入院を問わず，高齢患者が増加の一途をたどっている．厚生労働省の推計によると，2004年度において85歳以上の超高齢者は273.4万人と報告されている[1)]．高齢者に腎排泄型薬剤を投与する際，適正な用量を設定するため腎機能を正確に評価する必要がある．腎機能を表す指標として，糸球体濾過量には一般的に内因性クレアチニンクリアランス（以下Ccrと略す）が使われている．クリアランス試験には24時間蓄尿が必要であるが，時間を要することや被験者に排尿，蓄尿という負担があり繁雑であることから外来で測定することは容易ではない．このため血清クレアチニン値（以下Scrと略す）からCcrを推定するいくつかの数式が提案されている．しかしこれらの数式は実際に投薬の必要な諸疾患を有する高齢者に当てはめる際，筋肉量の減少などのためScrによるCcr推定値と実測したCcrがかけ離れた値を取ることがある．外来の超高齢患者においても適切な薬物療法を行うためには腎機能を正確に評価する必要がある．このため種々の推定式による相関を調べどの推定式が最もよく超高齢者に適合するか検討を行った．

## 対象及び方法

杏林大学病院高齢医学科に2004年9月から2006年1月の間に入院した60歳以上の症例のうち，短期入院や，蓄尿不可能症例を除外し，尿道留置カテーテルを使用している患者や蓄尿が可能と判断された症例全例を対象にした．疾患や治療による除外は設けず，脳血管障害，感染症，経口摂取不良，利尿剤，補液などの様々な基礎疾患，治療を有する高齢者（平均年齢82.9±8.6歳（男性82.0±8.8歳　女性83.8±8.3歳））例を対象に行った．男女比及び84歳以下と85歳以上の症例数に偏りはなかった（表1）．対象高齢者全体の平均Scrは1.31±0.87mg/dlであった．身体測定，血液検査，尿検査などを測定し24時間蓄尿によるCcrを計算した．なお，Ccrは未補正のものを使用した．安田の式[2)]，Cockcroft and Gaultの式[3)]（以下C&G式と略す），折田の式[4)]，Walserの式[5)]の推定値を算出し，それぞれ推定値と実測値の相関を回帰分析，相関係数の差の検定により解析し比較検討した．さらに，層別解析として，84歳までの前期及び後期高齢者群76名と，85歳以上の超高齢者67名について男女別に層別解析を行った．

また実測値と推定式からの値との一致を箱ヒゲ図で求

1) S. Hirayama：東京薬科大学
2) R. Kikuchi, S. Inoue, D. Tsukahara, Y. Suemitsu, Y. Kobayashi, Y. Sugiyama, H. Hasegawa, K. Kouzaki, K. Toba：杏林大学病院高齢医学科
3) G. Inoue：都東村山老人ホーム診療所内科
受付日：2006.4.18，採用日：2006.7.12

表1　対象年齢分布

| Age（歳） | n | | |
|---|---|---|---|
| | 男性 | 女性 | 全体 |
| ～84 | 42 | 34 | 76 |
| 85～ | 31 | 36 | 67 |
| 全体 | 73 | 70 | 143 |

め，値が外れ値となった症例については，患者の疾患や治療の背景，測定時の問題点について調査した．

本研究は，杏林大学高齢医学の入院に際して，CCr測定値を臨床研究に使用することを口頭で説明し同意を得て試行した．

(1) 安田の式

男性：Ccr（m$l$/min）＝（176－年齢）×体重（kg）÷（100×Scr（mg/100 m$l$））

女性：Ccr（m$l$/min）＝（158－年齢）×体重（kg）÷（100×Scr（mg/100 m$l$））

(2) Cockcroft and Gault の式

男性：Ccr（m$l$/min）＝（140－年齢）×体重（kg）÷（72×Scr（mg/100 m$l$））

女性：Ccr（m$l$/min）＝｛(140－年齢）×体重（kg）÷（72×Scr（mg/100 m$l$））｝×0.85

(3) 折田の式

男性：Ccr（m$l$/min）＝（－0.065×年齢－0.493×BMI＋33）÷（体重（kg）×Scr（mg/100 m$l$））×14.4

女性：Ccr（m$l$/min）＝（－0.052×年齢－0.202×BMI＋21）÷（体重（kg）×Scr（mg/100 m$l$））×14.4

(4) Walser の式

男性：Ccr（m$l$/min）＝7.57÷Scr（mM）－0.103×年齢＋0.096×体重（kg）－6.66

女性：Ccr（m$l$/min）＝6.06÷Scr（mM）－0.08×年齢＋0.08×体重（kg）－4.81

## 成　績

85歳未満の前期及び後期高齢者群において，安田，C&G，折田，Walser の推定値と24時間蓄尿による実測値の相関係数（r）は安田 r＝0.761，C&G　r＝0.761，折田 r＝0.693，Walser　r＝0.553 と安田の式，C&G 式で強い傾向があった．超高齢者群において，各々の推定式による推定値と実測値の相関係数は安田 r＝0.718，C&G r＝0.739，折田 r＝0.697，Walser r＝0.645 と，安田の式，C&G 式で相関が強い傾向があった（図1，図2）．超高齢者を男女に分け両群で各々の推定値と実測値の相関係数 r を比較したところ，男性で安田 r＝0.840，C&G r＝0.841，折田 r＝0.791，Walser　r＝0.736，女性で安田 r＝0.678，C&G　r＝0.690，折田 r＝0.667，Walser　r＝0.582 となり，男性に強い相関傾向があり，女性の相関係数は低かった（図3，図4）．また，超高齢者群において回帰係数を比較したところ，男性で安田＝0.796，C&G＝0.988，折田＝0.577，Walser＝0.375　女性で安田＝1.088，C&G＝1.262，折田＝0.776，Walser＝0.395 となった．

図5は超高齢者を男女で比較したものである．縦軸は実測値と推定値のずれの割合を示したもの（(実測値－推定値）×100/実測値）である．折田，Walser の式では，男女共に推定値が高く評価される傾向がある．

85歳以上の超高齢者での箱ひげ図における外れ値を検討し，実測値が高値となる6例の患者背景を調べた．輸液4例，利尿剤や Ca 拮抗薬など腎血流量を増加させる薬剤4例，腎不全2例，Scr 高値2例，心不全2例，CRP 高値2例であった．また，推定値が高値となる7例の患者背景を調べた．輸液5例，蓄尿不全または蓄尿少量4例，腎不全4例，癌3例，コントロール不良の糖尿病1例，胸水貯留，腹水貯留1例，肥満1例であった．

## 考　察

服用薬物数が多いほど薬剤有害作用の発現率は増加する傾向にある．また，加齢によってもその傾向は増加する[6]．その原因には加齢に伴う薬物動態学的・薬力学的な変化，多剤併用による相互作用，日常生活活動度（ADL）・認知機能の低下などが考えられるが，特に重大な原因として，腎機能の低下による相対的過量投与が挙げられる．Scr による腎機能の推定にはいくつか方法があるが高齢者，特に超高齢者になると筋肉量の低下により Scr が腎機能の低下と不相応な低値を示すことがしばしば見られる．Ccr 測定上の更なる問題点として正確な蓄尿の可否がある．加齢に伴う残尿，失禁の増加や患者自身による蓄尿もれなどにより，正確な24時間蓄尿が困難なことがある．1日尿量が少ないとき，Ccr 実測値と推定値のばらつきが大きいとの報告もある．今回は尿道留置カテーテルを使用している患者や蓄尿が可能と判断された患者の症例を対象とし，努めて正確な採尿を試みた．しかしながら，本来行うべきクリアランス法の実施には正確な蓄尿と安静を要し，判定に時間がかかるため実際の外来診療では実施困難なことが多い．従って Scr より Ccr を推定する種々の方法が提案されてきた．今回検討した安田の式，Cockcroft and Gault の式，折田の式，Walser の式は代表的な推定式であり Scr 値，性別，年齢，体重より Ccr を推定できる．C&G 式は欧米で最も広く用いられており欧米人によい相関を示して

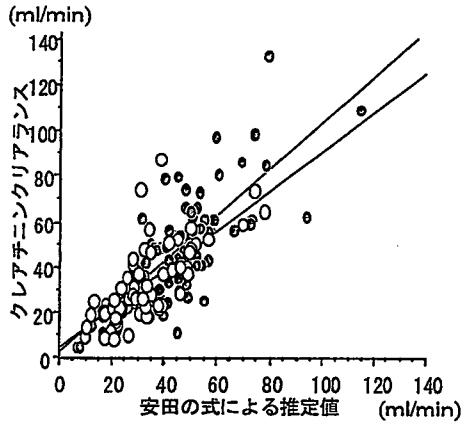


図1　安田の式　84歳以下と85歳以上の比較
○85歳以上；Y = 4.57 + 0.860X（r = 0.718）
●84歳以下；Y = 1.85 + 1.007X（r = 0.761）

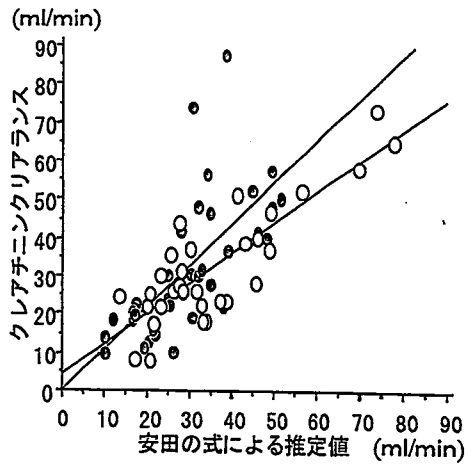


図3　安田の式　85歳以上の性差
○男性；回帰式 Y = 4.09 + 0.796X（r = 0.840）
●女性；回帰式 Y = 0.21 + 1.088X（r = 0.678）

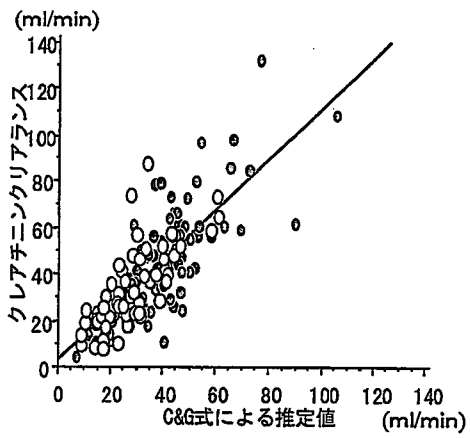


図2　C&G式　84歳以下と85歳以上の比較
○85歳以上；Y = 3.20 + 1.078X（r = 0.739）
●84歳以下；Y = 3.33 + 1.082X（r = 0.761）

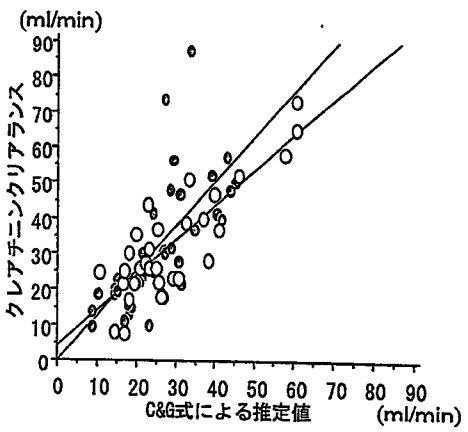


図4　C&G式　85歳以上の性差
○男性；回帰式 Y = 4.07 + 0.988X（r = 0.841）
●女性；回帰式 Y = − 0.09 + 1.262X（r = 0.690）

いる．今回の検討でも超高齢者における相関が0.739と最もよい相関を示した．この原因として日本人の体格が欧米化してきたことやC&G式作成時の対象年齢が18～92歳と超高齢者も含まれていること，作成時の対象症例数が多いことが考えられる．C&Gの式に対して他の3式はいずれもその後に発表されたもので，安田の式は1.4mg/dl以下の血清クレアチニン値を示す高齢者に限定して式を求めたもので，腎不全患者は含めずに高齢者の腎機能を推定しようとしたものである[2]．一方，Walserの式は血清クレアチニン値を2.0mg/dl以上におき，腎不全患者のみを対象としている[5]．堀尾らの式は腎疾患患者を対象として，推定式にBMIの項を加えて肥満の特徴加味して作成された[4]．したがって，今回の対象のように腎機能が広範囲に亘る場合，C-Gの式以外では，いずれもずれが出てしまう結果となったのは，式の作成経緯による要素も大きいと考えられる．

今回，臨床の現場では安定した時期より外来や急性期での腎機能評価を必要とするため，疾患による除外は設けず，脳血管障害，感染症，経口摂取不良，利尿剤，補液などの様々な基礎疾患，治療を有する高齢者を対象に行った．推定式と実測値の乖離に関して，実測値が大きい場合は，輸液や降圧剤など腎血流量を増加させる治療が関与していた場合が多かった．この場合は臨床的には大きな実害は考えられない．一方，実測値が推定式より小さい場合は，相対的な薬物の過量投与など安全管理上

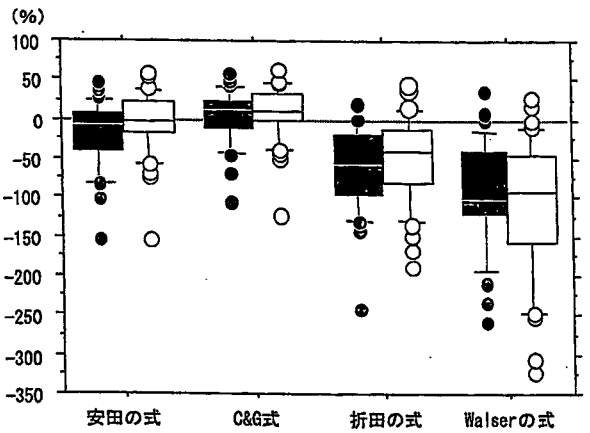


図5　超高齢者男女別において各推定式による推定値と実測値とのずれを箱ひげ図で％表示したもの
縦軸（実測値－推定値）×100/実測値
●男性
○女性

も問題となる．今回の検討では，腎不全，癌，乏尿，コントロール不良の糖尿病，胸水，腹水など複数の病態が重なる重症例で，有効循環血液量も日々変動しうる症例であった．このような症例に救急外来で遭遇した場合，血清クレアチニンから推定されるCcrの精度が低い可能性があることを銘記すべきであろう．Scrについては6.9までの高値も含まれているが，高値を除いた検討を行っても相関に大きな変化は見られなかった．全式において84歳までの前期及び後期高齢者群と85歳以上の超高齢者群に分け，相関を比較したところ，超高齢者群での相関が低い傾向にあり，超高齢者群での合併疾患の増加の影響が示唆される．これらを考慮しても，4種の推定式を比べると相関係数が最も高いC&G式が本邦超高齢者におけるCcr推定式として最適と考えられた．

超高齢者群を男女にわけC&Gの相関係数を比較したところ，男性0.841女性0.690と男性の相関が高い傾向にあった．また，回帰係数を比較したところ男性ではC&G式，女性では安田の式が1に近い値を示した．85歳以上の男性に安田の式を用いると過大評価する可能性があり，85歳以上の女性にC&G式を用いると過小評価する可能性がある．

一方，前期及び後期高齢者群の回帰係数を比較したところ男女ともに安田の式が1に近い値を示した．超高齢者の筋肉量について本邦での正確なデータは少ないが，中島らによれば70歳以降男性では上腕筋周囲，上腕筋面積が急速に減少するが女性ではほとんど変わらない[7]ことから女性の筋肉減少が時代とともに変化し，推定式の再構築が迫られている可能性があり，今後の検討課題と思われた．

本研究の限界として，膀胱留置カテーテルの適応がない蓄尿不可能症例を除外していることがあげられる．具体的には尿失禁症例や，認知症などが含まれるが，これらの症例に対してカテーテル留置を行ってクレアチニンクリアランスを測定し，高齢者全体に対するの推定式の良否を判断する研究は今後の課題であろう．

## 結　語

超高齢者において，正常値から腎不全を含む範囲の腎機能の判定に，24時間クレアチニンクリアランスの実測値と，すでに発表されている4つの式から求めた推定値とを比較して，超高齢者での推定式の有用性を検討した．4つの推定式のうち，C-Gの式はこの研究の目的にもっとも合致していた．一方，安田の式（高齢者，Scr: 1.4mg/dl以下），Wの式（Scr　2.0mg/dl以上）はいずれもその適用の目的の範囲で，また堀尾の式は腎疾患群内で有用と思われた．

全体として，臨床的に使用するうえでC&G式が最も優れているが，超高齢者への適用に当たっては，10%程度，推定値が低く求まるので，補正が望ましい．

今後超高齢者については，体格，サルコペニアの時代的変遷を考慮して改訂していく必要がある．

謝辞：本研究の一部は，長寿科学総合研究「縦断研究を基礎にした介護予防ガイドライン策定研究（H16痴呆骨折013；班長鳥羽研二），長寿医療研究事業「高齢者の安全な薬物療法ガイドライン策定研究（班長鳥羽研二）によった．

## 文　献

1) 厚生労働省ホームページ　平成17年度厚生統計要覧　総人口・日本人人口．性×年齢階級別．
2) 安田兵衛：腎機能の年齢的変化に関する研究．医学と生物学　1980; 101: 83-86.
3) Cockcroft DW, Gault MH: Prediction of Creatinine Clearance from Serum Creatinine. Nephron 1976; 16: 31-41.
4) Masaru Horio, Yoshimasa Orita, Shiro Manabe, Mitsuhiko Sakata, Megumu Fukunaga: Formula and Nomogram for Prediction Creatinine Clearance from Serum Creatinine Concentration. Clinical and Experimental Nephrology (1324-1751)　1997; 110-114.
5) Walser M, Drew HH, Guldan JL: Prediction of glomerular filtration rate from serum creatinine concentration in advanced chronic renal failure. Kidney International 1993; 44: 1145-1148.
6) 鳥羽研二，秋下雅弘，水野有三，江頭正人，金　承範，阿古潤哉ほか：薬剤起因性疾患．日老医誌　1999; 36: 181-185.
7) 中島久美子，秦　葭哉：身体組成としての筋肉量のアセスメント．日老医誌　2004; 42: 881-886.

# Creatinine clearance estimation in the extremely elderly subjects

Shunichi Hirayama[1], Reiko Kikuchi[2], Shinichiro Inoue[2], Daisuke Tsukahara[2], Yumi Suemitsu[2], Yoshio Kobayashi[2], Yoichi Sugiyama[2], Hiroshi Hasegawa[2], Koichi Kouzaki[2], Gosuke Inoue[3] and Kenji Toba[2]

## Abstract

**Background:** It has been reported that elderly outpatients take at least 6 different kinds of medication.

**Purpose:** To know which formula will best predict creatinine clearance, because 24-hour urine collection is difficult for elderly outpatients.

**Patients and Methods:** We compared four types of formulae (Cockcroft & Gault, Yasuda, Orita, Walser) to estimate creatinine clearance using serum creatinine of 143 elderly inpatients (73 men, 70 women, mean age 82.9±8.6 years old) including 67 extremely elderly people with various underlying diseases.

**Result:** The formula of Cockcroft and Gault showed the best correlation with creatinine clearance in the extremely elderly subjects ($r=0.74$) as well as in people under 85 years ($r=0.76$). However, the estimated values of the extremely elderly women were lower than actual creatinine clearance.

**Conclusion:** The formula of Cockcroft and Gault is the best predictive equation of creatinine clearance, except in the extremely elderly women.

Key words: *Extremely elderly, Creatinine clearance, Predicting formula, Cockcroft & Gault's formula, Yasuda's formula*
(Nippon Ronen Igakkai Zasshi 2007; 44: 90–94)

1) Tokyo University of Pharmacy and Life Science
2) Department of Geriatric Medicine, Kyorin University, School of Medicine
3) Department of Internal Medicine, Higashimurayama Nursing Home

ELSEVIER

Atherosclerosis xxx (2006) xxx–xxx

ATHEROSCLEROSIS

www.elsevier.com/locate/atherosclerosis

# Potent free radical scavenger, edaravone, suppresses oxidative stress-induced endothelial damage and early atherosclerosis

Hang Xi [a], Masahiro Akishita [b,*], Kumiko Nagai [a], Wei Yu [a], Hiroshi Hasegawa [a], Masato Eto [b], Koichi Kozaki [a], Kenji Toba [a]

[a] *Department of Geriatric Medicine, Kyorin University School of Medicine, Tokyo, Japan*

[b] *Department of Geriatric Medicine, Graduate School of Medicine, University of Tokyo, 7-3-1 Hongo, Bunkyo-ku, Tokyo 113-8655, Japan*

Received 28 November 2005; received in revised form 9 May 2006; accepted 19 May 2006

**Abstract**

*Objective:* Effects of potent free radical scavenger, edaravone, on oxidative stress-induced endothelial damage and early atherosclerosis were investigated using animal models and cultured cells.

*Methods and results:* Endothelial apoptosis was induced by 5-min intra-arterial exposure of a rat carotid artery with 0.01 mmol/L $H_2O_2$. Edaravone treatment (10 mg/kg i.p.) for 3 days suppressed endothelial apoptosis, as evaluated by chromatin staining of *en face* specimens at 24 h, by approximately 40%. Similarly, edaravone dose-dependently inhibited $H_2O_2$-induce apoptosis of cultured endothelial cells in parallel with the inhibition of 8-isoprostane formation, 4-hydroxy-2-nonenal (4-HNE) accumulation and VCAM-1 expression. Next, apolipoprotein-E knockout mice were fed a high-cholesterol diet for 4 weeks with edaravone (10 mg/kg i.p.) or vehicle treatment. Edaravone treatment decreased atherosclerotic lesions in the aortic sinus ($0.18 \pm 0.01$ to $0.09 \pm 0.01$ mm$^2$, $P < 0.001$) and descending aorta ($5.09 \pm 0.86$ to $1.75 \pm 0.41$ mm$^2$, $P < 0.05$), as evaluated by oil red O staining without influence on plasma lipid concentrations or blood pressure. Dihydroethidium labeling and cytochrome *c* reduction assay showed that superoxide anions in the aorta were suppressed by edaravone. Also, plasma 8-isoprostane concentrations and aortic nitrotyrosine, 4-HNE and VCAM-1 contents were decreased by edaravone treatment.

*Conclusions:* These results suggest that edaravone may be a useful therapeutic tool for early atherosclerosis, pending the clinical efficacy.


*Keywords:* Atherosclerosis; Reactive oxygen species; Free radical scavenger; Edaravone; 4-HNE; Apolipoprotein E knockout mouse

## 1. Introduction

Accumulating evidence has shown that stress-induced injury of vascular endothelial cells (ECs) is an initial event in the development of atherosclerosis [1]. In particular, oxidative stress has been implicated in endothelial injury caused by oxidized LDL and smoking as well as hypertension, diabetes and ischemia-reperfusion [1–3]. This notion is supported by the findings that the production of reactive oxygen species (ROS) is upregulated in vascular lesions [4,5], and that lesion formations such as endothelial dysfunction [6] and atherosclerosis [7] are accelerated by superoxide anion ($O_2^{\bullet -}$).

Experimental studies have shown the protective effects of antioxidants on atherosclerosis and endothelial injury. Dietary antioxidants were reported to preserve endothelial function [8,9] and inhibit atherosclerosis [10] in cholesterol-fed rabbits. In a well employed animal model of atherosclerosis, apolipoprotein E knockout (ApoE-KO) mouse fed a high fat diet, it has been shown that there was a significant increase in basal superoxide products [11,12], and that both $O_2^{\bullet -}$ levels and aortic lesion areas were attenuated by treatment with Vitamin E [11] or superoxide dismutase [13]. By contrast, it has been reported that elimination of NAD(P)H oxidase [14] or disruption of its subunit p47phox [15] had no effect on lesion size in ApoE-KO mice. Clinical experiments have

* Corresponding author. Tel.: +81 3 5800 8832; fax: +81 3 5800 8831.
*E-mail address:* akishita-tky@umin.ac.jp (M. Akishita).

0021-9150/$ – see front matter © 2006 Elsevier Ireland Ltd. All rights reserved.
doi:10.1016/j.atherosclerosis.2006.05.040

also shown that antioxidants such as Vitamins C and E can ameliorate endothelial dysfunction in patients with hypercholesterolemia or atherosclerosis [16,17], although recent clinical trials have failed to prove the protective effects of Vitamin E on cardiovascular events in patients with risk factors [18] and in healthy subjects [19].

Edaravone is a potent free radical scavenger that has been clinically used to reduce the neuronal damage following ischemic stroke [20]. Edaravone has promising property to quench hydroxyl radical ($^{\bullet}OH$) and show inhibitory effects on peroxynitrite ($ONOO^-$) and both water-soluble and lipid-soluble peroxyl radical ($LOO^{\bullet}$) [21,22]. Accordingly, this compound exerts a wide range of antioxidant activity on ROS beyond the effects of water-soluble or lipid-soluble antioxidant vitamins. Based on this idea, we hypothesized that edaravone would inhibit the process of atherosclerosis.

To test this hypothesis, we investigated the effects of edaravone in two experimental models. First, we examined whether edaravone could inhibit hydrogen peroxide ($H_2O_2$)-induced EC apoptosis in a rat model [23] and cultured ECs. Second, we examined whether edaravone could suppress the atherosclerotic lesion formation in ApoE-KO mice.

## 2. Methods

### 2.1. Animals

Male Wistar rats aged 10–12 weeks (Japan Clea), and male C57BL/6 mice and ApoE-KO mice on C57BL/6 background aged 4–6 weeks (Jackson Laboratory) were used in this study. All of the experimental protocols were approved by the Animal Research Committee of the Kyorin University School of Medicine.

### 2.2. $H_2O_2$-induced EC apoptosis in rats and in culture

EC apoptosis was induced by 5-min intra-arterial treatment of a rat carotid artery with 0.01 mmol/L $H_2O_2$ as previously described [23]. Briefly, edaravone (3-methyl-1-phenyl-2-pyrazolin-5-one; 3 or 10 mg/kg; donated by Mitsubishi Pharma Corporation, Japan) or its vehicle was intraperitoneally injected daily for 3 days before $H_2O_2$ treatment. A catheter was placed in the common carotid artery via the external carotid artery. The lumen was flushed with saline, replaced with 0.01 mmol/L $H_2O_2$ diluted with saline for 5 min and recovered. At 24 h after $H_2O_2$ treatment, EC apoptosis was evaluated by chromatin staining of *en face* specimens of the carotid artery using Hoechst 33342 dye. Apoptotic cells were identified by their typical morphological appearance; chromatin condensation, nuclear fragmentation, or apoptotic bodies. The numbers of apoptotic cells and intact cells were counted in 10 high-power fields for each specimen by an observer blinded to the treatment group.

Apoptosis of ECs isolated from a bovine carotid artery was induced as previously described [24]. Briefly, subconfluent ECs were pretreated for 24 h with culture medium containing edaravone or vehicle. After washing twice with Hank's balanced salt solution, the cells were exposed to $H_2O_2$ (0.2 mmol/L) diluted in Hank's balanced salt solution for 1.5 h at 37 °C to induce apoptosis. Then ECs were cultured in culture medium containing edaravone or vehicle until assay. Apoptosis was evaluated at 24 h after $H_2O_2$ treatment as histone-associated DNA fragments using a photometric enzyme immunoassay (Cell Death Detection ELISA, Roche), according to the manufacturer's instructions.

### 2.3. Atherosclerosis in ApoE-KO mice

ApoE-KO mice received a high-cholesterol diet (1% cholesterol, 10% fat in CE-2 standard diet; Japan Clea) for 4 weeks. Simultaneously, edaravone (10 mg/kg) or its vehicle was intra-peritoneally injected daily throughout the experiments. Body weight and systolic blood pressure were recorded every week in a conscious state by the tail cuff method (BP-98A; Softron, Tokyo).

At 4 weeks of treatment, mice were sacrificed with an overdose of diethyl ether and perfusion-fixed. Atherosclerotic lesions in the aortic sinus were quantified according to the method described previously [25]. We also measured the surface area of atherosclerotic lesions in the whole descending aorta including the abdominal aorta just proximal to the iliac bifurcation. *En face* specimens of the descending aorta were stained with oil red O, photographed and analyzed using the NIH image software. Total cholesterol, high-density lipoprotein cholesterol and low-density lipoprotein cholesterol in mice plasma were determined by a commercial laboratory (SRL, Japan).

### 2.4. Measurement of ROS

Aortic samples for ROS measurements were prepared separately from those for atherosclerosis evaluation. At 4 weeks of treatment, ApoE-KO mice were sacrificed with $CO_2$ inhalation. Descending aortas were rapidly removed and placed into chilled modified Krebs/HEPES buffer. C57BL/6 mice fed a standard diet were also used as the control. To determine superoxide production *in situ*, frozen cross-sections of the aorta were stained with 10 μmol/L dihydroethidium (DHE; Molecular Probes), followed by fluorescent microscopy [26]. Also, superoxide production in aortic rings was quantified using the superoxide dismutase-inhibitable cytochrome *c* reduction assay as previously described [27]. Immunohistochemical detection of 3-nitrotyrosine in the aorta was visualized by diaminobenzidine as reported previously [28].

Intracellular production of superoxide anions was measured using DHE as described previously [29], and the intensity values were calculated using the Metamorph software [24]. Concentrations of 8-isoprostane (8-iso prostaglandin

$F_{2\alpha}$) in the culture supernatants and mouse plasma were measured using a commercially available EIA kit (Cayman Chemical). Culture supernatants were directly applied to EIA, while plasma was applied to EIA after solid phase extraction purification according to the manufacturer's instructions.

### 2.5. Western blotting

Western blotting was performed as previously described [30], to detect the expression of VCAM-1 and 4-HNE in cultured ECs and mouse aortas. Descending aortas were prepared as described in ROS measurements. The antibodies used in this study were anti-4-HNE monoclonal antibody (JalCA, Shizuoka, Japan), anti-VCAM-1 polyclonal antibody (Santa Cruz Biotechnology) and anti-3-nitrotyrosine monoclonal antibody (Upstate). Densitometric analysis was performed using an image scanner and the NIH software.

### 2.6. Data analysis

All values are express as mean ± S.E.M. Data were analyzed using one-factor ANOVA. If a statistically significant effect was found, Newman–Keuls' test was performed to isolate the difference between the groups. Differences with a value of $P < 0.05$ were considered statistically significant.

## 3. Results

### 3.1. Effects of edaravone on $H_2O_2$-induced EC apoptosis and ROS

As shown in Fig. 1A, edaravone dose-dependently inhibited EC apoptosis in culture, which was induced 24 h after $H_2O_2$ treatment. Edaravone was then employed in a rat model of $H_2O_2$-induced EC apoptosis. Consistent with the *in vitro* experiment, edaravone of 10 mg/kg/day decreased EC apoptosis of the rat carotid artery by approximately 40% (Fig. 1B).

We next examined whether edaravone decreased ROS production in the process of $H_2O_2$-induced EC apoptosis. For this purpose, DHE fluorescent, a marker of intracellular production of superoxide anions, release of 8-isoprostane into the culture supernatants and accumulation of 4-HNE, a pivotal end-product of lipid peroxidation [31], were measured using cultured ECs. We also examined the expression of VCAM-1 as a marker of endothelial injury or activation [32]. Edaravone decreased DHE fluorescent, 8-isoprostane formation and VCAM-1 expression at 3 h after $H_2O_2$ treatment in a dose-dependent manner (Fig. 2A–C). As shown in Fig. 2D, multiple bands showing 4-HNE-Michael protein adducts [33,34] were accumulated after $H_2O_2$ treatment in a time-dependent manner. Consequently, the effect of edaravone on 4-HNE expression was examined at 3 h after $H_2O_2$ treatment (4.5 h after $H_2O_2$ was initially added). Edaravone decreased 4-HNE expression in a dose dependent manner.

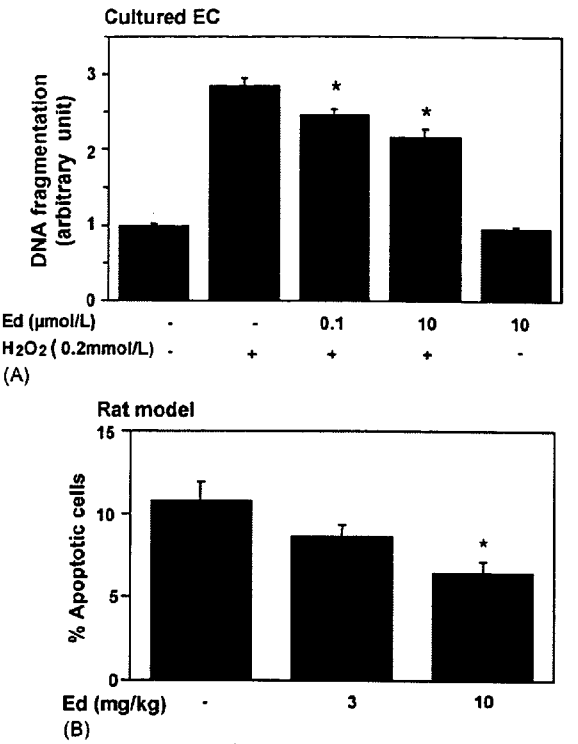


Fig. 1. Effects of edaravone (Ed) on $H_2O_2$-induced EC apoptosis in culture (A) and in a rat model (B). (A) Ed or its vehicle was added to the culture medium 24 h before $H_2O_2$ treatment until assay. EC apoptosis was evaluated 24 h after $H_2O_2$ treatment (0.2 mmol/L) by means of DNA fragmentation. Values are expressed as mean ± S.E.M. ($n = 3$). $^*P < 0.05$ vs. $H_2O_2$ (+) + Ed (−). (B) Ed or its vehicle was intraperitoneally injected once a day for 3 days before $H_2O_2$ treatment. At 24 h after $H_2O_2$ treatment, apoptotic ECs were counted per high power field and the ratio of the apoptotic cell number to the intact cells was calculated using *en face* specimens of the carotid artery stained with Hoechst 33342. Values are expressed as mean ± S.E.M. ($n = 7$). $^*P < 0.05$ vs. vehicle.

### 3.2. Effects of edaravone on atherosclerotic lesions and ROS in ApoE-KO mice

In the next set of experiments, we examined whether edaravone could suppress the atherosclerotic lesions in ApoE-KO mice fed a high cholesterol diet for 4 weeks. As shown in Fig. 3A and B, atheromatous lesions both in the aortic sinus and the descending aorta were smaller in mice treated with 10 mg/kg/day edaravone than in those with vehicle. This dose of edaravone did not influence body weight, blood pressure or plasma LDL and HDL cholesterol levels (Table 1).

Then, we examined whether the anti-atherogenic effects of edaravone were associated with the decrease in ROS production. Peroxynitrite formation was assessed as 3-nitrotyrosine accumulation in the aorta [28]. Both immunohistochemistry and Western blotting showed that edaravone inhibited nitrotyrosine accumulation in the aorta of ApoE-KO mice (Fig. 4A(a) and A(b)). Superoxide production *in situ* was examined using DHE staining of the descend-

Table 1
Body weight, blood pressure and plasma lipid levels in ApoE-KO mice treated with edaravone or vehicle

| | Vehicle | Edaravone |
|---|---|---|
| Body weight (g) | 21.4 ± 0.5 | 21.0 ± 0.5 |
| Systolic blood pressure (mmHg) | 106 ± 2 | 103 ± 3 |
| Total cholesterol (mg/dL) | 1967 ± 38 | 1872 ± 66 |
| HDL cholesterol (mg/dL) | 66 ± 6 | 82 ± 9 |
| LDL cholesterol (mg/dL) | 602 ± 24 | 602 ± 12 |

The values are shown as mean ± S.E. ($n = 14$). There were no significant differences in the values between the two groups.

ing aorta. As shown in Fig. 4B, ethidium fluorescence, which was amplified in ApoE-KO mice, was decreased by edaravone treatment. A quantitative analysis by the superoxide dismutase-inhibitable cytochrome *c* reduction assay revealed that $O_2^{\bullet -}$ levels in aortic rings of ApoE-KO mice were decreased by 43% in edaravone-treated ApoE-KO mice compared to those in vehicle-treated mice (Fig. 4C). Consistent with these results, plasma 8-isoprostane levels and 4-HNE expression in the descending aorta, both of which were elevated in ApoE-KO mice compared to

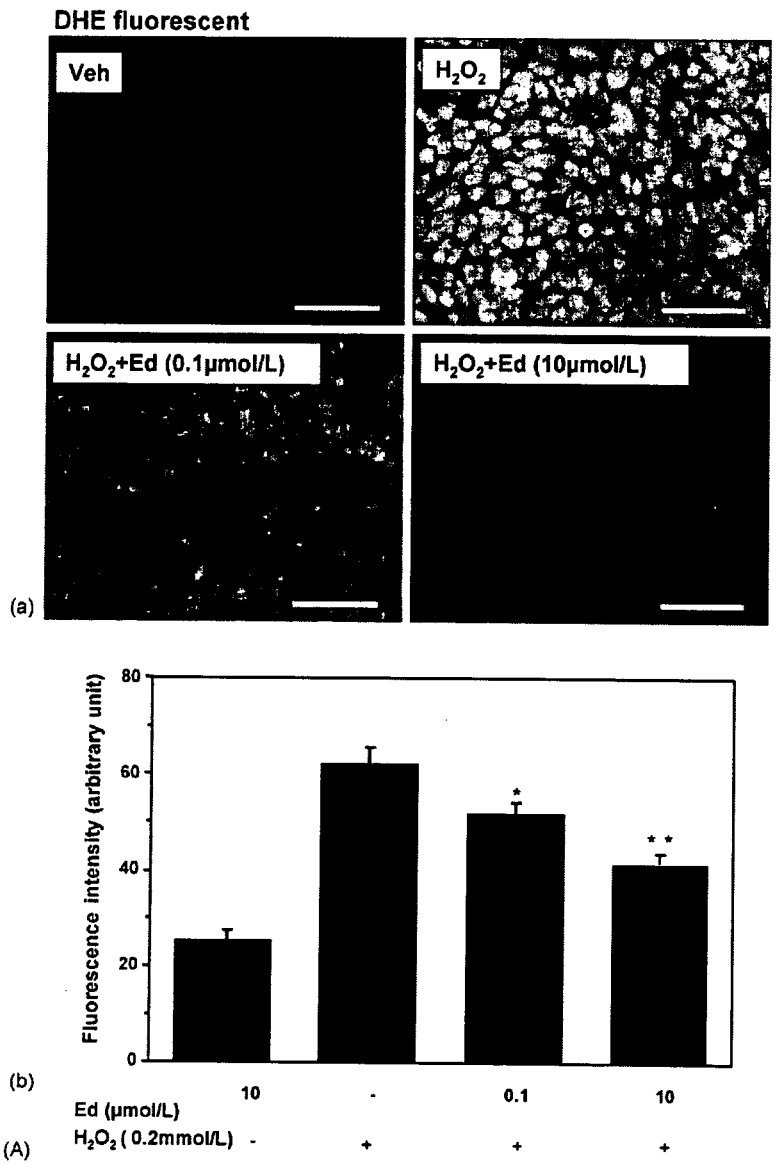


Fig. 2. Effects of edaravone (Ed) on DHE fluorescent (A) and 8-isoprostane formation (B), VCAM-1 expression (C) and 4-HNE expression (D) in cultured EC. Ed or its vehicle was added to the culture medium 24 h before $H_2O_2$ treatment until assay. DHE fluorescent ($n = 6$), 8-isoprostane concentration ($n = 3$) and VCAM-1 expression ($n = 3$) in the cell lysate were measured 3 h after $H_2O_2$ treatment. Values are expressed as mean ± S.E.M. Time dependent changes of 4-HNE expression after $H_2O_2$ treatment was detected by Western blotting. Representative image showed that 4-HNE-Michael protein adducts were accumulated after treatment (D(a)). The major 97 kDa band was measured 4.5 h after $H_2O_2$ treatment in the presence or absence of edaravone (D(b)). Values are expressed as mean ± S.E.M. ($n = 3$). $^{*}P < 0.05$, $^{**}P < 0.01$ vs. $H_2O_2$ (+) + Ed (−).

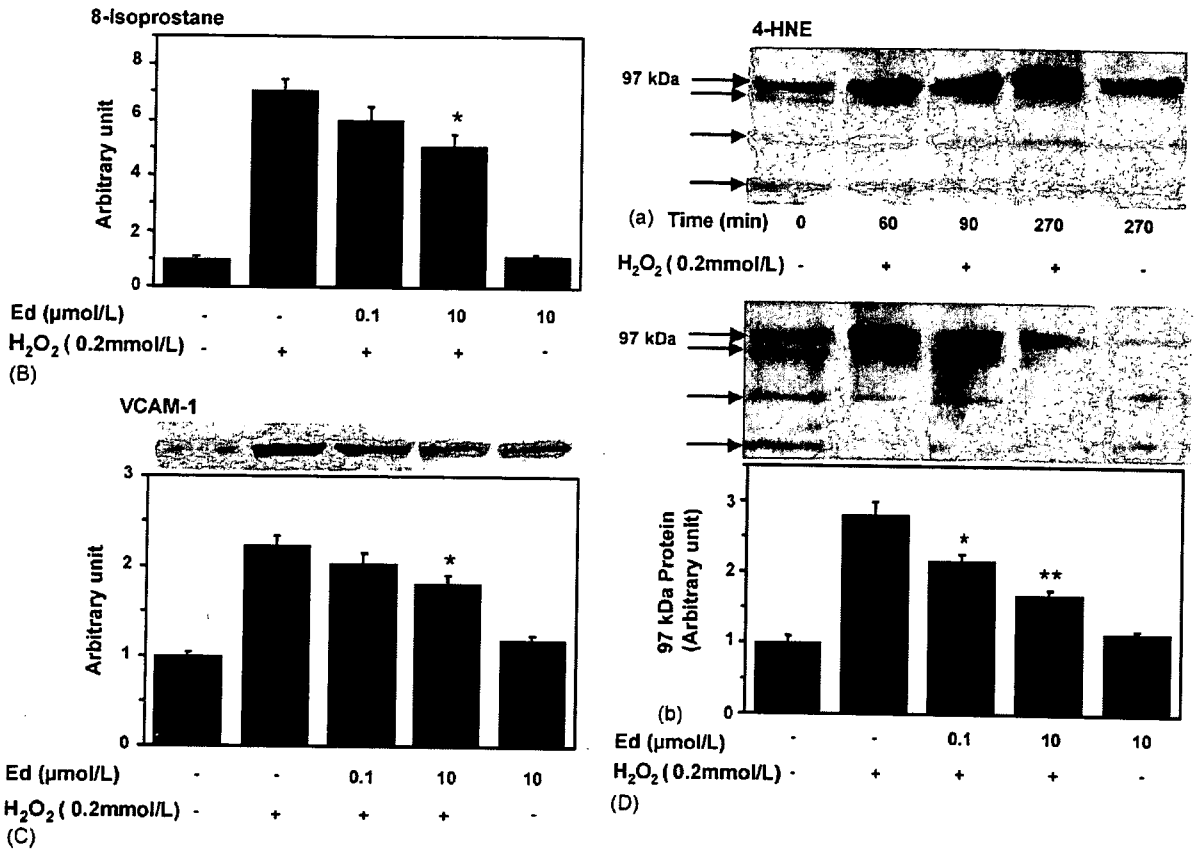


Fig. 2. (*Continued*).

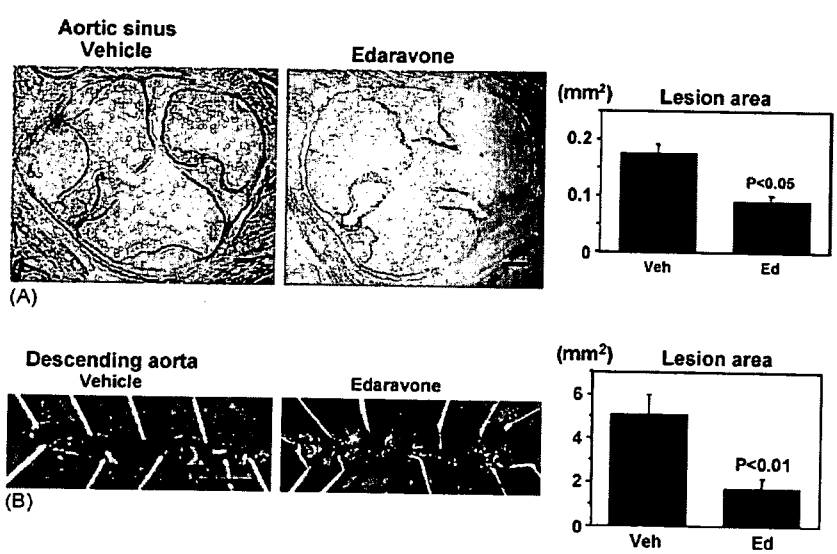


Fig. 3. Effects of edaravone on atherosclerotic lesion in ApoE-KO mice. ApoE-KO mice were fed a high-cholesterol diet for 4 weeks with the administration of edaravone (10 mg/kg daily) or its vehicle by i.p. injection. (A) Oil red O-stained cross-sections of the aortic sinus (bar = 100 μm) and morphometric analysis of the lesions are shown. (B) Oil red O-stained *en face* specimens of the descending aorta (bar = 5 mm) and morphometric analysis of the lesions are shown. Values are expressed as mean ± S.E.M. ($n = 14$).

those in wild-type C57BL/6 mice fed a normal chow, were decreased by edaravone treatment (Fig. 4D and E). Finally, the increase in VCAM-1 expression in the aorta of ApoE-KO mice was attenuated by edaravone as well (Fig. 4F).

## 4. Discussion

A number of studies have shown that ROS contribute to the pathogenesis of endothelial dysfunction and atherosclerosis formation. In addition to $O_2^{\bullet -}$ that is predominantly pro-

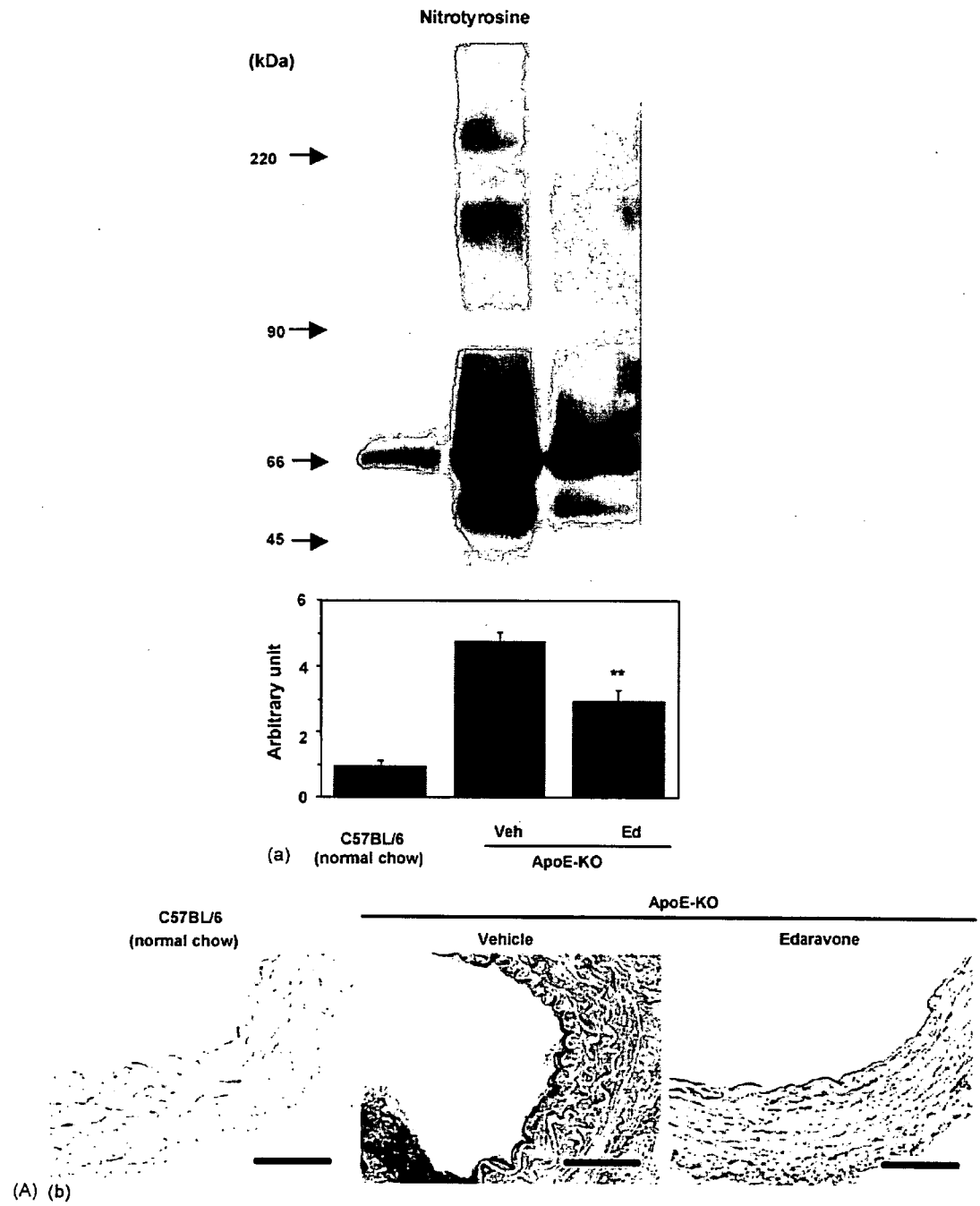


Fig. 4. Effects of edaravone (Ed) on ROS production (A–E) and VCAM-1 expression (F) in ApoE-KO mice. (A) Nitrotyrosine contents in the aorta was examined by Western blot analysis (A(a), $n=6$) and immunohistochemistry (A(b)). Bar = 50 μm. (B) Fresh-frozen cross-sections of the aorta were stained with DHE, and representative fluorescent micrographs are shown (bar = 100 μm). (C) Superoxide anion in aortic rings was determined using SOD inhibitable-cytochrome *c* reduction assay ($n=6$). (D) 8-Isoprostane level in mouse plasma was measured with EIA ($n=6$). (E and F) Representative Western blotting for 4-HNE (97 kDa band) and VCAM-1 expression in the aorta and densitometric analysis are shown ($n=3$). Values are expressed as mean ± S.E.M. $^{*}P<0.05$, $^{**}P<0.01$ vs. vehicle (Veh). C57/BL6 mice fed a normal chow serve as the control.